Comparative analysis on the bactericidal components formation of air plasma jets driven by DC glow discharge and dielectric-barrier discharge

A. Kazak[1], A. Kirillov[1], L. Simonchik[1], O. Stepanova[2], A. Astafiev[3] and M. Pinchuk[3]

[1]*Institute of Physics of NAS of Belarus, Minsk, Belarus*
[2]*St. Petersburg State University, Saint Petersburg, Russia*
[3]*Institute for Electrophysics and Electric Power of Russian Academy of Sciences, Saint Petersburg, Russia*

Abstract: Air plasma jets driven by a DC atmospheric pressure glow discharge (APGD) and dielectric barrier discharge (DBD) have been studied because they are known as bacterial inhibitors. The concentrations of inactivation components were determined by the IR absorption spectroscopy. The mechanisms and zones of formation of the main bactericidal components of the APGD (NO, NO_2, HNO_2) and DBD (O_3) air plasma jets have been revealed.

Keywords: atmospheric pressure plasma jet, glow discharge, dielectric-barrier discharge, absorption spectroscopy, bactericidal components, plasma-chemical reactions.

1. Introduction

Atmospheric pressure plasma jets (APPJ) are widely studied due to their prospective capabilities to be used in plasma medicine technologies [1]. Basic applications of APPJ are linked with that they can transfer numerous chemical and biological active species from a discharge region to a treated object. A bactericidal number of active species (reactive oxygen and nitrogen species, or ROS and RNS) is efficiently generated in the case of using air as a feeding gas.

To produce APPJ from the ambient air, we used two different types of atmospheric pressure discharges: DC glow discharge (APGD) developed by the Belarusian group of the paper’s authors [2-4] and dielectric barrier discharge (DBD) studied by the Russian scientific group [5, 6]. Since the discharges have a various nature of existence, different chemical gas composition of the air plasma jets can be expected.

Comparative analysis of the composition, mechanisms and zones of bactericidal components formation of air plasma jets based on APGD and DBD was performed.

2. Generation of air plasma jets

To generate a glow discharge and dielectric-barrier discharge in air flow, two gas discharge cells with the same geometry have been fabricated. They provide the same gas-dynamics conditions due to the identical geometrical sizes.

A quartz tube with an inner diameter of 7.5 mm was equipped by a cylindrical copper electrode of 4 mm in diameter fixed along the center line of the tube. In the case of DC glow discharge it serves as a cathode, whereas a copper nozzle with the outlet hole of 1.5 mm diameter was used as an anode firmly pressed to the polished edge of the quartz tube. In the case of DBD, the central cylindrical electrode was under the high voltage. As a second (grounded) electrode, a copper foil strip with the wideness of 7 mm wrapped on the outer side of the tube was used. The outlet of the tube was closed with a dielectric nozzle with a 1.5 mm diameter hole. A draft of the both discharge cells is presented in Fig. 1. An interelectrode gap was 0.7 mm for both cases. A gas flow rate was equal to 5 l/min.

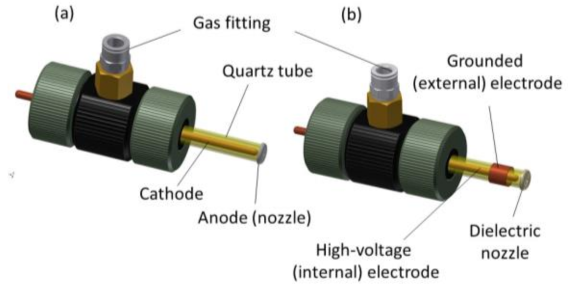

Fig. 1. Draft of the discharge cells to obtain plasma jets of a DC glow (a) and dielectric barrier (b) discharges.

To feed a DC glow discharge, DC voltage of up to 1 kV was applied to the electrode system through a limiting resistor of 29 kΩ. It provides discharge current up 20 to 40 mA. The discharge currents and voltages were recorded by means of two true-RMS multimeters. In addition, to monitor fast-changing processes, the same values were recorded with an oscilloscope.

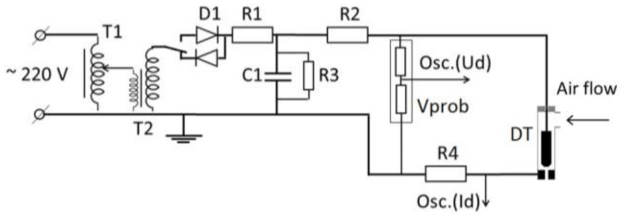

Fig. 2. Electrical schematic of DC atmospheric pressure glow discharge plasma jet generation.

Current-voltage characteristic (CVC) of APGD in air without air blowing through the discharge cell show in

Fig.3 curve a. This CVC corresponds to the CVC of the classical atmospheric pressure glow discharge in the air. When air is blown at 5 L/min through the discharge cell, the current-voltage characteristic is shifted (curve b). In this case, in the region of small currents (less than 15 mA), the discharge breaks into a spark or ceases to exist.

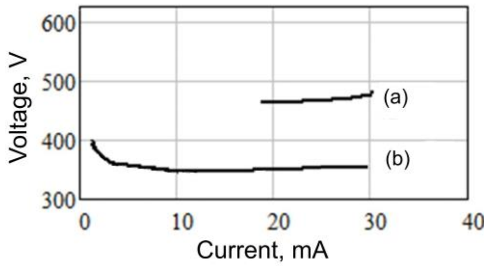

a – in a stationary air medium; b – in the air flow.

Fig. 3. Current-voltage characteristics of the APGD in air.

In the case of DBD generation, a 26 kHz sinusoidal voltage power supply was used. Electric parameters were measured with a current shunt of 1 kΩ and 1:9090 voltage divider. Fig. 4 shows an electrical schematic of the DBD plasma jet generation setup.

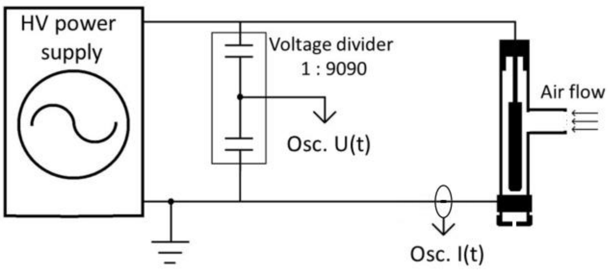

Fig. 4. Electrical schematic of DBD plasma jet generation.

Oscillograms of the measured voltage and current signals are shown in Fig. 5.

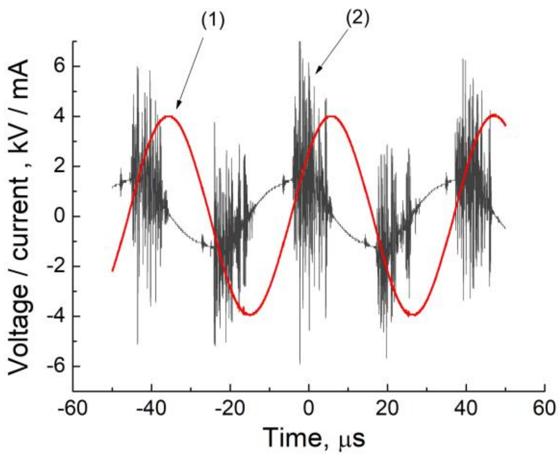

Fig. 5. Discharge voltage (1) and current (2) probe signals.

Discharge voltage applied to the inner electrode has an amplitude value of 4 kV. A typical measured current signal includes a displacement current (a sinusoidal component) and the numerous peaks of conduction current, which indicate microdischarges with the amplitude up to 6 mA.

3. Absorption spectroscopy measurements

The absorption spectra are registered using a Fourier IR spectrometer Nexus (Thermo-Nicolet) with a gas cell 186-0305 (Perkin-Elmer) with a controlled optical path from 11 cm up to 10 m and with germanium windows. A spectrum registration is carried out using a DTGS detector with a spectral range of 600-4000 cm^{-1} at a resolution of 2 cm^{-1} after 128 scans. The optical path of the gas cell was chosen to be equal to 135 cm. Gas was collected into the cell with a tube of 3.5 mm in diameter. The tube was placed along the jet axis and parallel to the gas flow direction.

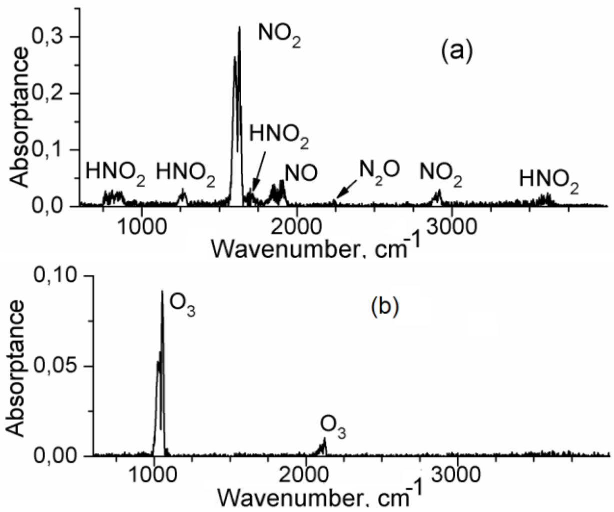

Fig. 6. The absorption spectra for air plasma jets driven by APGD (a) and DBD (b) at the gas collection near the nozzle.

The spectra were recorded at different distances from the nozzle. In all the spectra, bands corresponding to CO_2 and H_2O molecules were observed, which were removed from the spectra by subtracting the air spectra through the cell without discharge breakdown. Fig. 6 shows the characteristic spectra of bactericidal components for APGD and DBD air plasma jets recorded at 0 cm from the nozzle. The presence of molecules in the spectrum of RNSs, such as NO, NO_2, HNO_2, is typical for APGD jet spectra. In comparison with the APGD jets, DBD jet spectra have ozone bands. Concentrations of the bactericidal components of the jets were determined by comparing the experimental absorption spectra with ones calculated using the HITRAN spectral data base [7]. Concentrations near the nozzle are 400, 310, 85 ppm for NO, NO_2, HNO_2, respectively and 70 ppm for O_3.

4. Results and discussion

The formation of various bactericidal components in air plasma jets driven by APGD and DBD is due to the difference in the plasma parameters of these discharges. At a discharge current of 30 mA, the gas temperature of the APGD plasma is 1600 K and the typical density of ~ 10^{12}–10^{13} cm^{-3} and average electron energy of 1 eV [8]. In DBD discharge, the gas temperature slightly exceeds the room temperature, and the average electron energy reaches several eV.

Considering the characteristics of plasma APGD, the analysis shows that the formation of N, O, and OH in plasma-chemical reaction involving electrons is more efficient than thermal dissociation of nitrogen, oxygen and water molecules. Moreover, this is the true for dielectric-barrier discharges. Atomic oxygen creates conditions for the production of ozone by the reaction:

$$O + O_2 + M \rightarrow O_3 + M \qquad M = O_2, N_2.$$

Due to the low gas temperature (~ 330 K) in DBD, the dissociation of ozone molecules is insignificant

$$O_3 + M \rightarrow O + O_2 + M \qquad M = O_2, N_2$$

and most of the ozone molecules formed in the DBD are saved in a plasma jet.

On the contrary, due to the very low energy of breaking the bond of the ozone molecule of 1.04 eV, an intensive process of dissociation is observed in APGD at a temperature of 1600 K, resulting in a negligible O_3 concentration. In the plasma of APGD, the formation of nitrogen monoxide is more efficient. It should be noted that the temperature of 1600 K is not enough to correctly describe the formation of NO in the framework of the extended Zeldovich thermal mechanism

$$N_2 + O \leftrightarrow NO + N,$$

$$N + O_2 \leftrightarrow NO + O,$$

$$N + OH \leftrightarrow NO + H$$

and kinetic analysis is required in view of plasma-chemical reactions.

Since the conditions for the thermal dissociation of nitrogen dioxide and nitrous acid molecules are provided in the active zone of the discharge, the increase in their concentrations in the reactions

$$NO + O + M \rightarrow NO_2 + M + h\upsilon,$$

$$NO + OH + M \rightarrow HNO_2 + M$$

starts outside the APGD zone with decreasing temperature downstream. The NO_2 production in the three-body chemiluminescence reaction with the participation of NO and O is accompanied by intense emission of the jet in the spectral range of 400-800 nm.

In the far low-temperature zone of the jet, where the dissociation process is not effective, formation a noticeable concentration of ozone does not occur because the previously the fast three-body reaction of NO_2 formation "takes away" the oxygen atoms necessary to produce O_3. The nascent ozone molecules die in collisions with molecules of nitrogen monoxide and nitrogen dioxide, already having a significant concentration.

5. Acknowledgments

The work was financially supported by the Belarusian Republican Foundation for Fundamental Research (projects F17RM-050, F18SRBG-001) and the Russian Foundation for Basic Research (project 17-58-04052).

6. References

[1] J Winter, R Brandenburg and K-D Weltmann, Plasma Sources Sci. Technol. **24**, 064001 (2015)

[2] A.A. Kirillov, A.V. Paulava, Y.A. Safronau, L.V. Simonchik, Appl. Phys., **5**, 52–55 (2013)

[3] A.V. Kazak, A.A. Kirillov, L.V. Simonchik, O.E. Nezhvinskaya, N.V. Dudchik, Plasma Medicine **7** (2), 109-115 (2017)

[4] V.I. Arkhipenko, A.V. Kazak, A.A. Kirillov, L.V. Simonchik, V.V. Shkurko, High Temp. Mater. Process. **22** (4), 273–278 (2018)

[5] O. Stepanova, O. Rybalchenko, M. Pinchuk, A. Astafiev, O. Orlova, V. Spodobin, A. Kudryavtsev, Plasma Medicine, **7** (3), 187-200 (2017)

[6] M. Pinchuk, O. Stepanova, N. Kurakina, V. Spodobin, Journal of Physics: Conference Series **830** (1), 012060 (2017)

[7] The HITRAN Database [Electronic resource]. – Mode of access: http://www.cfa.harvard.edu/HITRAN/. – Date of access: 03.02.2015.

[8] V.I. Arkhipenko, A.A. Kirillov, L.V. Simonchik, Ya.A. Safronau, S.M. Zgirouski. Eur. Phys. J. D, **66** (10), 252 (2012)